doi:10.1093/jmcb/mjv033
Published online June 1, 2015

Article

Post-translational *O*-GlcNAcylation is essential for nuclear pore integrity and maintenance of the pore selectivity filter

Yanping Zhu[1,2], Ta-Wei Liu[1,2], Zarina Madden[1], Scott A. Yuzwa[2], Kelsey Murray[2], Samy Cecioni[1], Natasha Zachara[3], and David J. Vocadlo[1,2,*]

[1] Department of Chemistry, Simon Fraser University, Burnaby, British Columbia V5A 1S6, Canada
[2] Department of Molecular Biology and Biochemistry, Simon Fraser University, Burnaby, British Columbia V5A 1S6, Canada
[3] Department of Biological Chemistry, Johns Hopkins University Medical School, Baltimore, MD 21205, USA
* Correspondence to: David J. Vocadlo, E-mail: dvocadlo@sfu.ca

***O*-glycosylation of the nuclear pore complex (NPC) by *O*-linked *N*-acetylglucosamine (*O*-GlcNAc) is conserved within metazoans. Many nucleoporins (Nups) comprising the NPC are constitutively *O*-GlcNAcylated, but the functional role of this modification remains enigmatic. We show that loss of *O*-GlcNAc, induced by either inhibition of *O*-GlcNAc transferase (OGT) or deletion of the gene encoding OGT, leads to decreased cellular levels of a number of natively *O*-GlcNAcylated Nups. Loss of *O*-GlcNAc enables increased ubiquitination of these Nups and their increased proteasomal degradation. The decreased half-life of these deglycosylated Nups manifests in their gradual loss from the NPC and a downstream malfunction of the nuclear pore selective permeability barrier in both dividing and post-mitotic cells. These findings define a critical role of *O*-GlcNAc modification of the NPC in maintaining its composition and the function of the selectivity filter. The results implicate NPC glycosylation as a regulator of NPC function and reveal the role of conserved glycosylation of the NPC among metazoans.**

Keywords: post-translational modification, *O*-GlcNAcylation, nuclear pore complex, protein stability, ubiquitination, nucleoporin, glycosylation

Introduction

The nuclear pore complex (NPC) is a multiprotein assembly embedded within the nuclear envelope (NE) that forms an aqueous channel connecting the nucleus and cytoplasm (Hoelz et al., 2011). Thirty component proteins form this elaborate 8-fold symmetric 125-MDa channel, and these proteins are categorized as belonging to distinct groups (Cronshaw et al., 2002; Elad et al., 2009; Hoelz et al., 2011; Maimon et al., 2012). Transmembrane Nups, which are embedded within the NE, fix the pore in place to the membrane. Scaffolding Nups associate with the transmembrane protein anchor to form several rings that serve as docking sites for peripheral Nups. Peripheral Nups form several features including filaments that extend into the cytoplasm, a basket-like structure that extends into the nucleoplasm, and the selective permeability barrier found in the center of the channel (D'Angelo et al., 2009; Jovanovic-Talisman et al., 2009; Raices and D'Angelo, 2012). This selectivity barrier is responsible for regulated passage of molecules larger than 60 kDa (Weis, 2003; Alber et al., 2007; Debler et al., 2008; Brohawn et al., 2009) and enabling regulated nucleocytoplasmic transport, which is the most recognized function of the NPC (Weis, 2002; Wente and Rout, 2010).

The NPC is being uncovered as a critical complex involved in many cellular processes including, for example, the regulation of genome architecture and gene expression (Capelson et al., 2010; Vaquerizas et al., 2010; Van de Vosse et al., 2013; Sood and Brickner, 2014), cell division (Makhnevych et al., 2003; Rodriguez-Bravo et al., 2014), and differentiation (Lupu et al., 2008; Asally et al., 2011; Raices and D'Angelo, 2012). Recent studies have uncovered a critical role for the NPC in aging of post-mitotic cells (D'Angelo et al., 2009). Notably in this regard, most scaffolding Nups have been shown to be extremely long-lived and do not either exchange or turn over in post-mitotic cells (Toyama et al., 2013). Due to the long lifetime of many pore components, cumulative insults can impair their function and lead to an age-related loss of cell compartmentalization, leakage of cytoplasmic proteins into the nucleoplasm, and eventual cell death (D'Angelo et al., 2009). These findings have positioned the NPC and its constituent components

Received January 18, 2015. Revised March 31, 2015. Accepted April 13, 2015.

as central players in cellular and organismal homeostasis (D'Angelo and Hetzer, 2008; Strambio-De-Castillia et al., 2010; Natalizio and Wente, 2013), making the mechanisms governing their maintenance and stability of interest.

One striking feature common to all metazoans is that their NPCs are extensively modified by nucleocytoplasmically disposed *N*-acetylglucosamine (GlcNAc) residues *O*-linked to serine and threonine residues (*O*-GlcNAc) (Li and Kohler, 2014). Eighteen out of 30 component proteins have been shown to be *O*-GlcNAc modified (Supplementary Table S1). These Nups, especially peripheral Nups, are constitutively modified with high stoichiometric levels of *O*-GlcNAc. Despite the NPC being found to be *O*-GlcNAcylated almost 30 years ago (Davis and Blobel, 1987; Hanover et al., 1987; Holt et al., 1987), the cellular roles of *O*-GlcNAc on this structure have remained enigmatic. Notably, Nups are among the best substrates of the glycosyltransferase responsible for glycosylation of nucleocytoplasmic proteins, *O*-GlcNAc transferase (OGT) (Kreppel et al., 1997; Lubas et al., 1997; Shen et al., 2012). *O*-GlcNAc is reversible and the removal of *O*-GlcNAc from the NPC and other proteins is mediated by a glycoside hydrolase known as *O*-GlcNAcase (OGA) (Dong and Hart, 1994; Gao et al., 2001). OGT and OGA act in concert to regulate the levels of *O*-GlcNAc within cells on proteins including those of the NPC (Vocadlo, 2012). The functional roles of *O*-GlcNAc on proteins are being gradually uncovered, and this modification has been implicated in various processes including regulation of gene expression and signaling, as well as pathological processes including cancer, aging, and neurodegeneration (Hart et al., 2011).

Although *O*-GlcNAc was found to be abundant especially on the NPC and its Nup components were reported a number of years ago to be extensively *O*-GlcNAc modified, the functional role of *O*-GlcNAc at the NPC remains unclear. Given that *O*-GlcNAc modification of the NPC is conserved among all metazoans studied to date, that Nups are excellent substrates for OGT, and that Nups bear a high stoichiometric level of *O*-GlcNAc, we hypothesized that *O*-GlcNAc likely plays a critical role in the functioning of the NPC. Because *O*-GlcNAc has been reported to influence the cellular levels of some proteins including various transcription factors (Han and Kudlow, 1997; Yang et al., 2001, 2006; Hardiville et al., 2010; Park et al., 2010), we hypothesized that *O*-GlcNAc might serve to regulate the stability of *O*-GlcNAc-modified Nups and so play a critical role in the integrity of the NPC within cells.

Here we address the role of *O*-GlcNAc on the mammalian NPC and representative members of both peripheral and scaffold Nups (D'Angelo et al., 2009; Hoelz et al., 2011). We find that reduction of *O*-GlcNAc levels leads to accelerated turnover of these Nups via the ubiquitin–proteasome pathway. *O*-GlcNAc modification of Nups hinders their ubiquitylation, and loss of *O*-GlcNAc accordingly increases ubiquitylation. The effect of this accelerated turnover is the time-dependent loss of these Nups from the NPC and a striking loss of integrity of the selective permeability barrier of the NPC in both dividing and post-mitotic cells. *O*-GlcNAc therefore plays a critical protective role in stabilizing the NPC to maintain integrity of its selectivity filter.

Results

Reduction of O-GlcNAc levels leads to decreases in the levels of nucleoporins

To test our hypothesis regarding the critical functional role of *O*-GlcNAc modification of the NPC, we first investigated the effectiveness and time dependence of two approaches to decrease *O*-GlcNAc levels on Nups. We recently reported an inhibitor of OGT termed Ac5SGlcNAc, which functions in various cell lines (Gloster et al., 2011). Additionally, we also recently generated mouse embryonic fibroblasts (MEFs) in which knockout of OGT can be induced (Kazemi et al., 2010). Activation of the Cre recombinase in these cells by tamoxifen leads to loss of the genomically-encoded floxed *ogt*. We verified in these $OGT^{F/Y}$ cells that cellular *O*-GlcNAc levels decreased significantly in a time-dependent manner following induction by 0.7 μM 4-hydroxytamoxifen (4HT) or treatment with 50 μM Ac5SGlcNAc (Figure 1A and B). Immunoprecipitation of Nup62 showed that this Nup also had significantly decreased *O*-GlcNAc levels (Figure 1C). This observation is consistent with global decreases in *O*-GlcNAc levels as well as the observed loss of *O*-GlcNAcylation on proteins at the nuclear membrane (Figure 1D). We analyzed OGT levels in these cells over several days by immunoblotting (Figure 1E and F) and found that OGT levels dropped upon treatment with 4HT and increased in cells treated with Ac5SGlcNAc, which is consistent with previous reports using these approaches to alter *O*-GlcNAc levels (Kazemi et al., 2010; Gloster et al., 2011). Because OGT has many interacting partners (Hanover et al., 2012; Ruan et al., 2012), using two different approaches to decrease *O*-GlcNAc levels is valuable. The concordance in the observed effects of these strategies cannot arise from changes in altered cellular levels of OGT and downstream effects on protein partners.

Following treatment of MEFs with 4HT or Ac5SGlcNAc, we analyzed cell lysates to establish the levels of several components of the NPC that are known to be *O*-GlcNAc modified. We observed a decrease in the levels of Nup62, which has been noted upon inhibition of OGT (Gloster et al., 2011) or knockdown of OGT (Mizuguchi-Hata et al., 2013). More broadly, we observed a time-dependent decrease in both peripheral Nups, including Nup62, Nup153, Nup214, and Nup358, as well as scaffold Nups Nup93 and Sec13 (Figure 2A–F and Supplementary Figure S1A–D). Nup93 has been identified as being glycosylated both in proteomic screens (Boyce et al., 2011) and by mapping an *O*-GlcNAc site to T96 (unpublished data). Because antibody mAb414 was raised against NPC proteins bearing *O*-GlcNAc, we wanted to address whether *O*-GlcNAc is part of the epitope recognized by this antibody. If this were the case, reduced *O*-GlcNAcylation could compromise mAb414 binding and confound interpretation of results dependent on its use. We assessed this possibility by parallel immunoblot analysis of *O*-GlcNAcylated and enzymatically de-*O*-GlcNAcylated Nup62 using mAb414. Nup62 was efficiently deglycosylated, as reflected by the band shift upon β-glucosaminidase digestion, and was recognized by mAb414 as efficiently as natively *O*-GlcNAcylated Nup62 (Supplementary Figure S1E). This result indicates that loss of *O*-GlcNAc does not influence the recognition of Nups by mAb414, providing support for the use of this antibody in the quantitative analyses performed here. We note that the

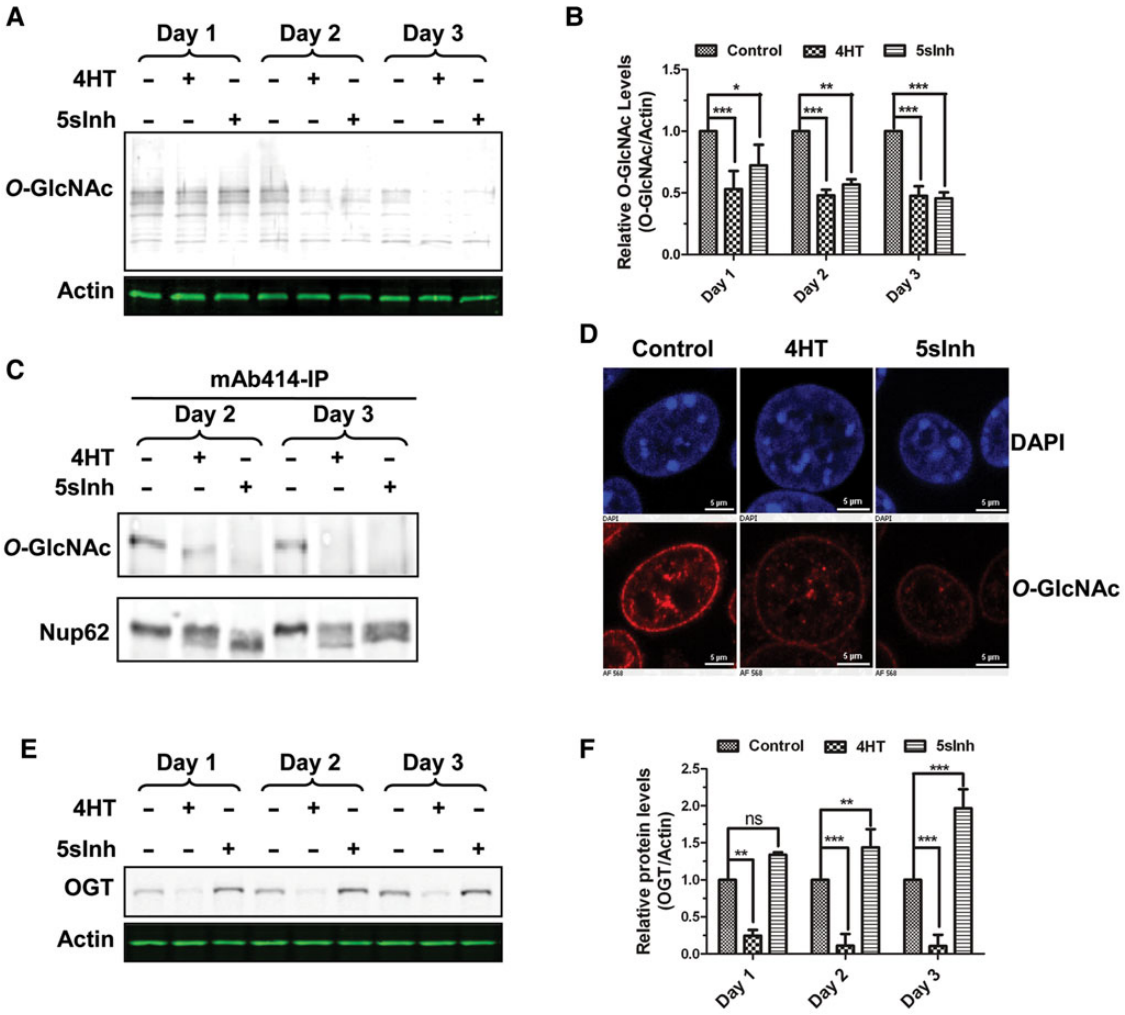

Figure 1 Reduction of *O*-GlcNAc levels by inducible OGT knockout or OGT inhibition. Western blot analysis of total cell lysates after inducing OGT knockout or Ac5SGlcNAc administration at 50 μM for different time periods. (**A**) *O*-GlcNAc (CTD110.6) blots. β-actin is shown as loading control. (**B**) Densitometry of immunoblot signals in **A** was quantified using Odyssey software (Li-Cor). Values were normalized to corresponding β-actin immunoblot signals, and then normalized to control. Error bars represent standard deviations (SD). *P*-values were derived from a two-way analysis of variance (ANOVA) comparing immunoblot signals from 4HT or 5sInh treatment with control ($n = 3$); $^{*}P < 0.05$, $^{**}P < 0.01$, $^{***}P < 0.001$, ns, not significant. (**C**) Nup62 was immunoprecipitated using antibody mAb414, and then blotted with *O*-GlcNAc antibody CTD110.6 or mAb414. (**D**) Immunofluorescent microscopy for detection of *O*-GlcNAc on nuclear envelope. Nuclei were isolated from cells after OGT knockout or inhibition for 5 days, fixed, and stained with CTD110.6. (**E** and **F**) OGT blots and densitometry of immunoblot signals.

levels of some pore proteins, such as Nup62 (Figure 2A and D), drop much more rapidly than others such as Sec13, which decreases only slightly after 5 days (Figure 2C and F). Notably, the band corresponding to Nup62 is shifted in a time-dependent manner upon treatment with 4HT or Ac5SGlcNAc (Figure 2A), consistent with the time-dependent loss of *O*-GlcNAc observed by anti-*O*-GlcNAc antibodies (Figure 1C). The results obtained using both OGT inhibition and OGT knockout are in accord, though the inhibitor has a more pronounced effect. Notably, levels of non-glycosylated nucleoporins, Nup107 and Nup133, and ribosome component RPS6 did not decrease following OGT inhibition or knockout (Supplementary Figure S2A), suggesting that the effect on stability of the affected Nups is not general to all proteins.

O-GlcNAc modification of nucleoporins affects their stability

OGT has been proposed to play a role in the regulation of gene expression (Fujiki et al., 2009; Gambetta et al., 2009; Sinclair et al., 2009; Love et al., 2010). However, using both qPCR and semi-quantitative RT–PCR, we found no effects on Nup mRNA levels when using either OGT knockout or inhibition (Figure 3), suggesting that decreased Nup levels are not mediated at the transcriptional level. To investigate whether decreased *O*-GlcNAc accelerated the degradation of these Nups, we used a pulse-chase strategy making use of the methionine analogue L-azidohomoalanine (AHA), which can be chemoselectively linked to biotin using a highly chemoselective chemical reaction known as the Staudinger ligation (Saxon and Bertozzi, 2000). Following overnight OGT inhibition or induction of

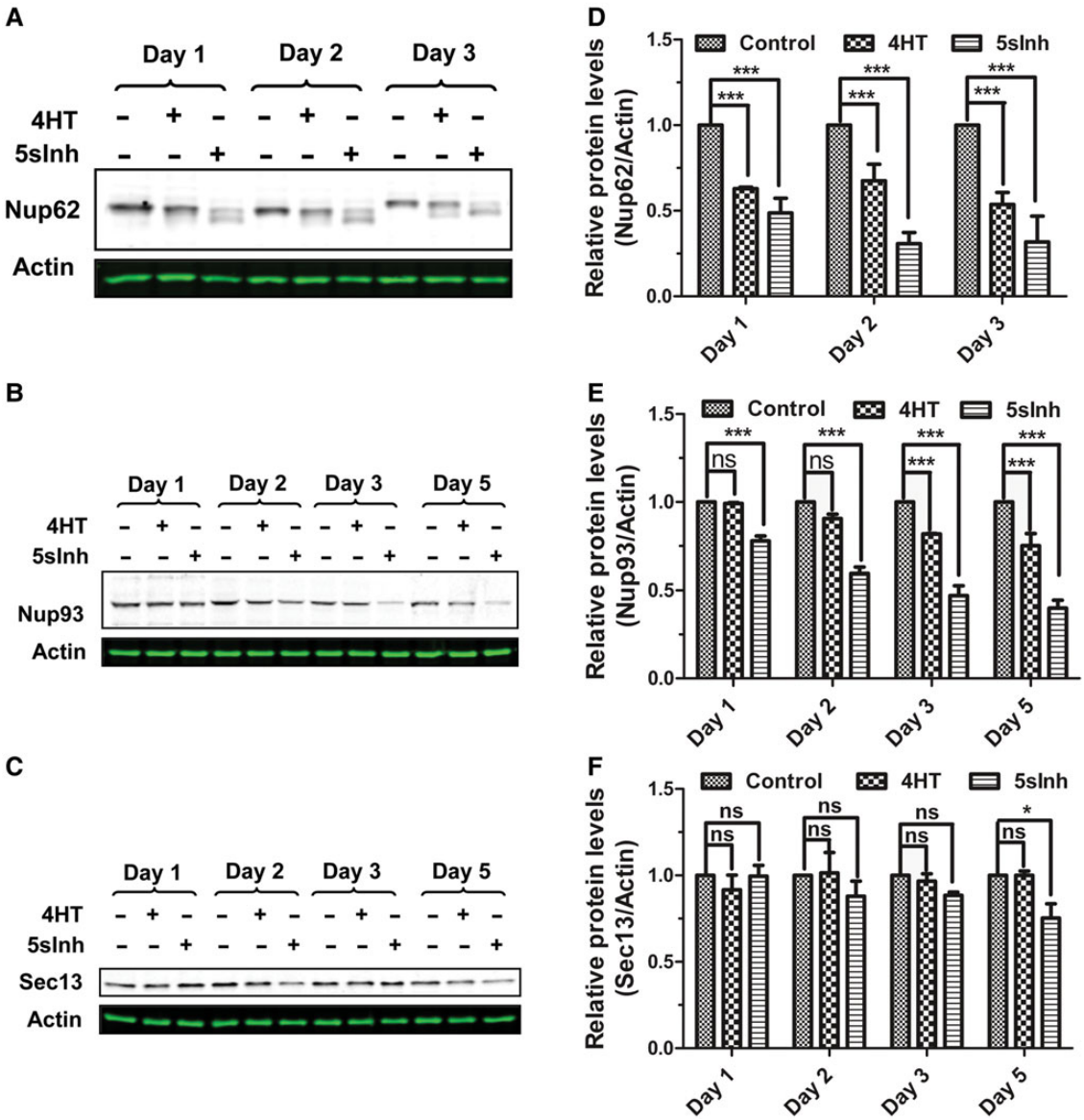

Figure 2 Reduction of *O*-GlcNAc levels affects the levels of Nups. Western blots of total cell lysates after inducing OGT knockout or Ac5SGlcNAc administration at 50 μM for different time periods. (**A**) Nup62 (mAb414) blots. (**B**) Nup93 blots. (**C**) Sec13 blots. β-actin is shown as loading control. (**D**–**F**) Densitometry of immunoblot signals in **A**–**C** was quantified using Odyssey software (Li-Cor). Values were normalized to corresponding β-actin immunoblot signals, and then normalized to control. Error bars represent SD. *P*-values were derived from a two-way analysis of variance (ANOVA) comparing immunoblot signals from 4HT or 5sInh treatment with control ($n = 3$); $^{*}P < 0.05$, $^{**}P < 0.01$, $^{***}P < 0.001$, ns, not significant.

knockout, cells were pulsed with AHA and then chased for different lengths of time with methionine. The entire AHA-containing proteome was tagged using a triarylphosphine-biotin probe (Saxon and Bertozzi, 2000), isolated using streptavidin agarose resin, and then probed by immunoblot.

We found that decreased *O*-GlcNAc levels accelerated the degradation of Nup62 and Nup93 (Figure 4A, B, F, and G). The effect was more pronounced for Nup62 than Nup93, but was significant by either knockout or inhibition of OGT. To validate these results, we used the cycloheximide chase approach. Two days after starting inhibition or induction of knockout of OGT, MEFs cells were treated with cycloheximide to stop protein biosynthesis. The levels of the Nups of interest were then followed as a function of time by immunoblot analysis. All Nups tested, including Nup62, Nup93, Nup153, Nup214, Nup358, and Sec13, turned over more quickly following OGT knockout or inhibition compared with control cells (Supplementary Figure S3). These data are consistent with those obtained from AHA pulse-chase experiments, and they collectively support the proposal that loss of *O*-GlcNAc leads to an increased rate of degradation of the Nups studied here, which manifests as

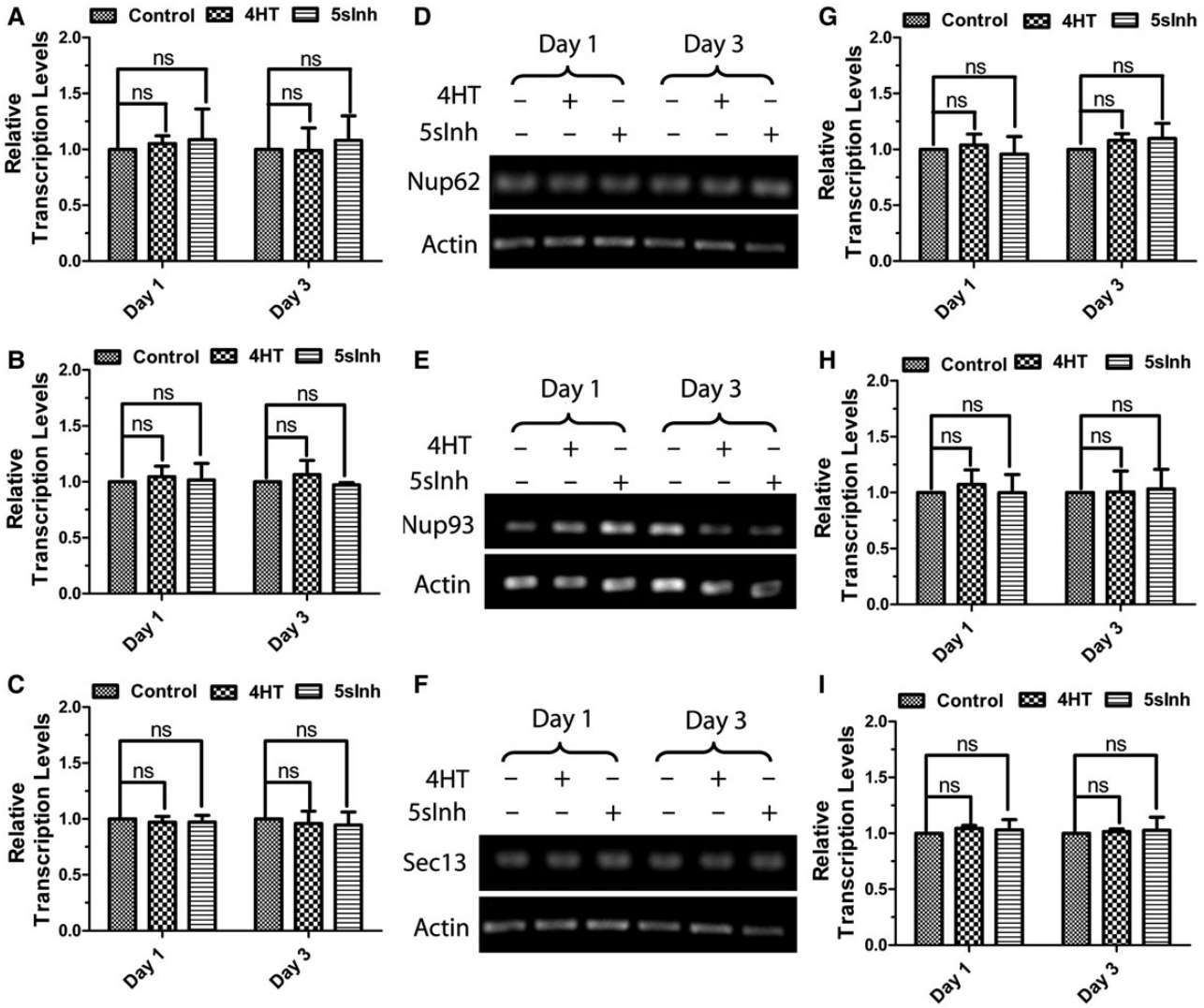

Figure 3 Reduction of *O*-GlcNAc levels does not affect the transcription of Nups. Nup transcription levels in MEF cells after inducing OGT knockout or OGT inhibition for different time periods (Day 1 and 3) were analyzed by Q-PCR ($n = 3$). (**A**) Nup62 transcription levels. (**B**) Nup93 transcription levels. (**C**) Sec13 transcription levels. Nup transcription levels in MEF cells after OGT knockout or inhibition for different time periods (Day 1 and 3) were analyzed by semi-quantitative RT–PCR. β-actin is shown as endogenous control. (**D**) Nup62 transcription levels. (**E**) Nup93 transcription levels. (**F**) Sec13 transcription levels. (**G**–**I**) Densitometry of band intensity in **D**–**F** was quantified using ImageJ. Nup transcript levels were normalized to β-actin mRNA levels, and then normalized to controls ($n = 3$). Ns, not significant.

decreased levels of these Nups within cells.

To determine which degradation pathway is involved, we evaluated the effect of the proteasome inhibitor, N-Acetyl-L-leucyl-L-leucyl-L-norleucinal (LLnL) (Vinitsky et al., 1992) on these Nups. We found that following OGT knockout or inhibition, Nup62 levels did not decrease but slightly increased within cells treated with LLnL, compared with LLnL-treated control cells having functional OGT (Figure 4C and H). The same effects were observed for all other natively glycosylated Nups, including Nup153, Nup214, and Nup358 (Supplementary Figure S1A–D). To clarify how decreased *O*-GlcNAc levels accelerated proteasomal degradation of *O*-GlcNAc-modified Nups, we immunoprecipitated Nup62 from control cells, OGT knockout cells, and cells treated with Ac5SGlcNAc to assess its ubiquitination status. Though no change in the extent of Nup62 ubiquitination was observed, we speculated that its rapid proteolysis might occur following ubiquitylation. We therefore treated cells with LLnL and deubiquitinase inhibitor PR619 (Altun et al., 2011; Tian et al., 2011) in tandem to prevent degradation of ubiquitinylated proteins. Immunoblot analysis of Nup62 immunoprecipitated from these cells revealed significantly higher levels of ubiquitin upon OGT inhibition or knockout, compared with control cells (Figure 4D and I). These data support that reduction of Nup *O*-GlcNAc modification facilitates ubiquitylation, which in turn leads to their rapid proteasomal degradation.

Decreased cellular *O*-GlcNAcylation might exert direct or indirect effects on ubiquitylation of Nups. In a direct mechanism, *O*-GlcNAcylation of Nups could act to hinder their ubiquitylation, and loss of Nup glycosylation could therefore enable their

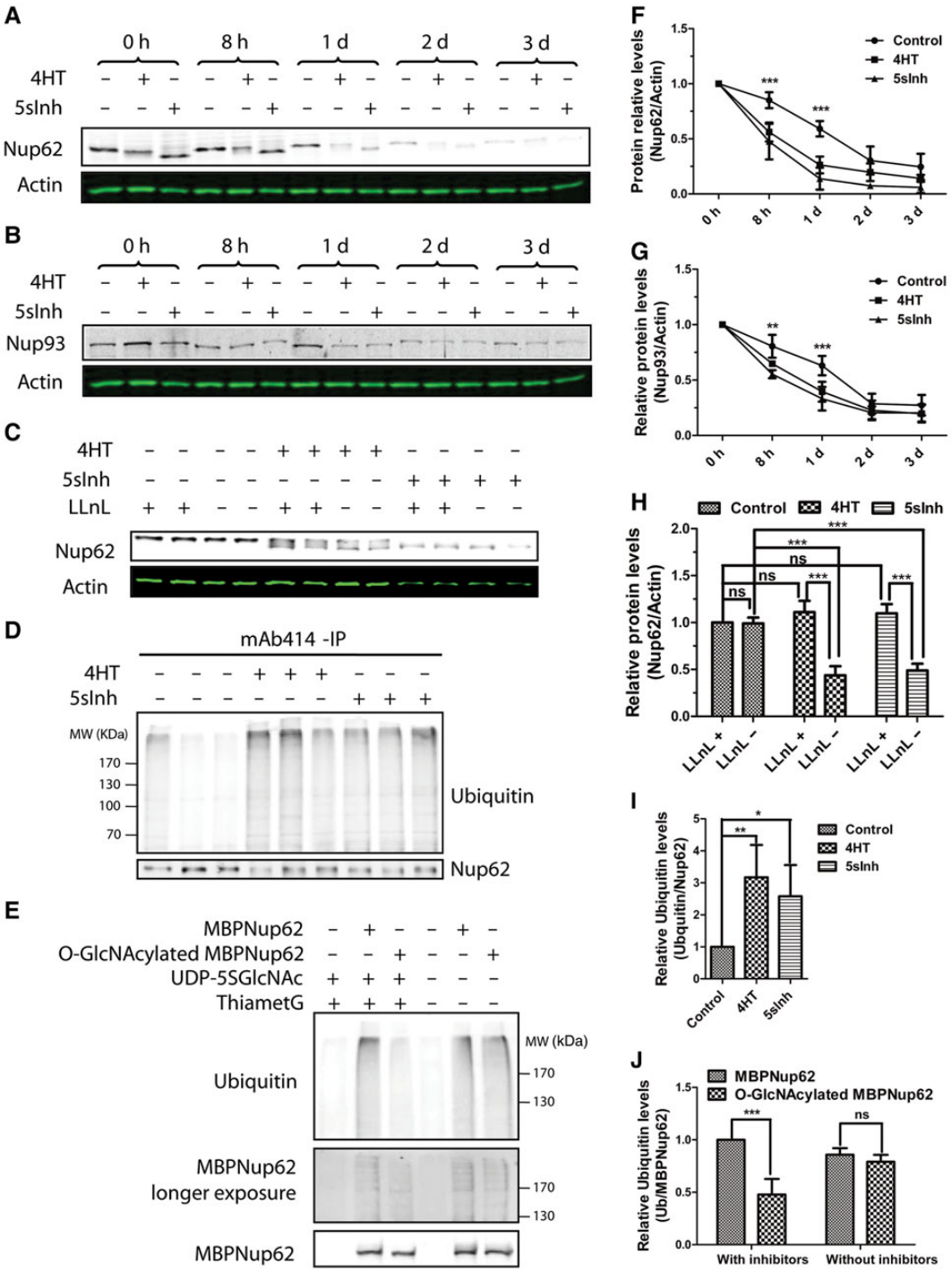

Figure 4 *O*-GlcNAc stabilizes Nups through disturbing the ubiquitin–proteasomal degradation pathway. Western blots of L-azidohomoalanine (AHA)-labeled proteome from pulse-chase experiments using anti-Nup62 antibody (mAb414) (**A**) or anti-Nup93 antibody (**B**). β-actin is shown as loading control. (**C**) Western blots of total cell lysates from cells treated with or without proteasome inhibitor LLnL for Nup62. After OGT knockout or inhibition for 2 days, MEFs cells were incubated with or without 30 μM LLnL and harvested 5 h later. (**D**) Immunoblots for detection of ubiquitin on Nup62 immunoprecipitated using mAb414. After OGT knockout or inhibition for 2 days, MEFs cells were incubated with 30 μM LLnL and 5 μM PR619, and harvested 5 h later. Nup62 is shown as loading control. (**E**) *In vitro* ubiquitination assays. Reaction without MBPNup62 protein was set up as control. The middle panel showed the ladders of MBPNup62 bands with different extent of polyubiquitylation. (**F**–**J**) Densitometry of immunoblot signals in **A**–**E** was quantified using Odyssey software (Li-Cor). Values were normalized to corresponding β-actin immunoblot signals, and then normalized to the corresponding values at 0 h time point in **F** and **G** ($n = 3$) or to the value of control with LLnL administration in **H** ($n = 3$). In **I** and **J**, values were normalized to corresponding Nup62 immunoblot signals, and then normalized to control ($n = 3$).

ubiquitylation as observed. In an indirect mechanism, decreased cellular *O*-GlcNAcylation might activate the ubiquitylation machinery, which would lead to the increased ubiquitin modification and accelerate the downstream degradation of Nups. We first assessed the total ubiquitylation levels in cells, and found no significant difference between cells with decreased *O*-GlcNAc and control cells, suggesting that reduced *O*-GlcNAcylation did not cause obvious alterations in global ubiquitylation (Supplementary Figure S2D). To assess whether the direct effect is operative, we carried out *in vitro* ubiquitylation experiments using Nup62 as a model Nup. MBP-tagged Nup62 (MBPNup62), which can be stably expressed and does not aggregate spontaneously, was recombinantly expressed in *E. coli*. Following purification, MBPNup62 was *O*-GlcNAcylated *in vitro* using OGT and re-purified. *O*-GlcNAc-modified and unmodified MBPNup62 proteins were incubated with rabbit reticulocyte lysate (RRL) as a source of active ubiquitylating enzymes in the presence of both proteasome and deubiquitinase inhibitors. Since these lysates are known to have active OGA and OGT, and are able to *O*-GlcNAcylate Nups (Starr and Hanover, 1990) and other proteins (Iyer et al., 2003; Wells et al., 2011), we also blocked OGA and OGT activities using inhibitors to ensure static *O*-GlcNAc levels during the assays. When OGT and OGA activity was blocked, we observed that ubiquitylation of unmodified MBP-Nup62 was markedly higher than that of *O*-GlcNAcylated MBPNup62 (Figure 4E and J). In assays where OGT and OGA were active in the lysates, a trend to lower ubiquitination of *O*-GlcNAcylated MBPNup62 was observed, but the effect was not significant. Next, we expressed mutant FLAG-tagged Nup62, with its known *O*-GlcNAc sites mutated to alanine in order to decrease Nup62 *O*-GlcNAcylation. These mutant and double-mutant proteins all showed reductions in their levels of *O*-GlcNAcylation, either as a trend or significantly (Figure 5A and B). These Nup62

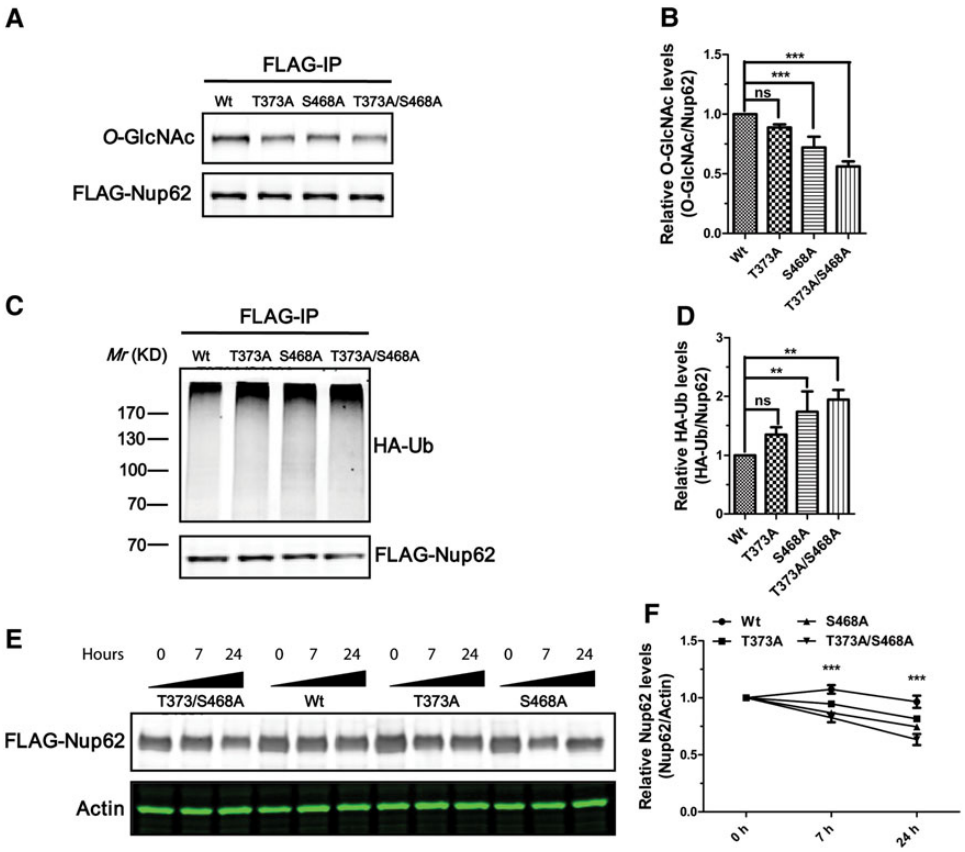

Figure 5 Mutagenesis of known *O*-GlcNAc sites suggests that *O*-GlcNAc increases Nup stability by decreasing ubiquitination. (**A**) *O*-GlcNAcylation of Nup62 wild-type (wt) and mutants expressed within HEK cells by transfection. (**B**) The immunoreactivity observed in **A** was quantified using Odyssey software. Values of *O*-GlcNAc signals were normalized to corresponding FLAG-Nup62 immunoreactive signals, and then normalized to the corresponding wild-type protein. *P*-values were derived from one-way analysis of variance ($n = 3$). (**C**) Ubiquitination of Nup62. Nup62 was isolated by immunoprecipitation from cells overexpressing both 3XFLAG-Nup62 and HA-Ubiquitin, and treated with or without OGT inhibitor. (**D**) The immunoblot signals in **C** were quantified using Odyssey software (Li-Cor). Values of HA-Ub signals were normalized to corresponding FLAG immunoblot signals, and then normalized to wt ($n = 3$). (**E**) Cycloheximide-chase experiments showed that the degradation rate of *O*-GlcNAc site mutants was greater than that of wild-type Nup62. Two days after the transfection, cycloheximide was added to the culture media to a final concentration of 100 μg/ml. Cells were harvested at the indicated time points. β-actin was used as a loading control. (**F**) Densitometry of immunoblot signals in **E** was quantified using Odyssey software (Li-Cor). Values were normalized to corresponding β-actin immunoblot signals, and then normalized to the corresponding values at 0 h time point ($n = 3$). Data were analyzed using two-way analysis of variance.

mutant proteins were more extensively ubiquitinated in cells and showed significantly increased degradation rates (Figure 5C–F). While not addressing indirect effects of *O*-GlcNAcylation on Nup ubiquitylation within cells, these results reveal that *O*-GlcNAc plays a direct role in moderating ubiquitylation of Nup62 and its proteasomal degradation. Accordingly, a direct mechanism may also be operative for other glycosylated Nups that show decreased stability in response to decreased *O*-GlcNAcylation.

Decreased O-GlcNAcylation compromises the selective permeability barrier but not active transport through the nuclear pore

We next examined whether the natively *O*-GlcNAcylated Nups were lost from the Nup pool within the NPC or other protein pools in the nucleus or cytoplasm. Nuclei isolated from cells treated with Ac5SGlcNAc or OGT knockout were analyzed by immunocytochemistry. We found that OGT immunoreactivity was greatly reduced in cells where the *ogt* gene had been excised and was much higher in nuclei from cells treated with Ac5SGlcNAc compared with control nuclei (Figure 6A), which is consistent with the results from immunoblot analyses of total cell lysates (Figure 1E and F). *O*-GlcNAc immunoreactivity was much lower in nuclei from cells with OGT knockout or inhibition compared with control nuclei (Figure 6B), indicating that these treatments effectively decreased *O*-GlcNAc levels both within nuclei and at the nuclear membrane, despite OGT inhibition leading to increased OGT protein levels. Levels of Nup93 and FG-rich Nups, namely Nup62, Nup153, Nup214, and Nup358 assessed using mAb414, within the nuclear envelope were all dramatically reduced by both OGT inhibition and knockout (Figure 6A, B, D, and E), corresponding to the decreases in total levels of these Nups at the nuclear membrane (Supplementary Figure S4A and B). In contrast, Sec13 levels at the nuclear membrane were unchanged by decreased cellular *O*-GlcNAc levels (Figure 6C and F and Supplementary Figure S4A and B). These results suggest that, once incorporated within the NPC, scaffold Nups such as Sec13 may not be significantly destabilized following the loss of *O*-GlcNAc, and the number of NPCs may therefore remain unchanged. To determine whether the reduced mAb414 staining of the nuclear envelope stemmed from decreased numbers of NPCs at the membrane, we analyzed the nuclear surface of mAb414-labeled control cells and cells with OGT knockout or inhibition. Nuclear pores from cells having decreased *O*-GlcNAcylation displayed much lower intensity of staining (Supplementary Figure S4C). However, when digitally increasing the brightness, it was apparent that there was comparable density of NPCs on the nuclear membranes of control cells and those having reduced *O*-GlcNAc levels (Supplementary Figure S4C and D). Furthermore, levels of non-glycosylated Nups within the nuclear envelope, Nup107 and Nup133, did not decrease following OGT inhibition or knockout (Supplementary Figure S2B and C). These data indicate that decreased *O*-GlcNAc does not contribute to a loss of nuclear pores from the nuclear membrane but rather to a loss of certain specific natively *O*-GlcNAcylated pore components.

We speculated that the gradual time-dependent loss of these Nups from the NPC would compromise NPC function. One critical activity of the NPC is to serve as a selective permeability barrier to control transport of macromolecules between the nucleus and cytoplasm. We therefore set out to evaluate whether loss of *O*-GlcNAc and decreased incorporation of Nups would compromise the NPC selectivity barrier using inert fluorescent dextrans of different molecular weights in a dextran exclusion assay (Lenart and Ellenberg, 2006). This assay enables the integrity of nuclei to be studied, and is reportedly more sensitive than active transportation assays for evaluating NPC function (Lenart et al., 2003). Dextran molecules larger than 60 kDa cannot pass through the selectivity barrier of the NPC and are excluded from intact nuclei (Lenart et al., 2003). Failure of the NPC permeability barrier enables passage of dextran molecules of 70 kDa. But 500 kDa dextrans cannot pass through the NPC even when the selectivity barrier is compromised. Only when perforations are present in the nuclear envelope are 500 kDa dextrans able to pass into the nucleus (Stehno-Bittel et al., 1995; Galy et al., 2003). Therefore, this assay allows perforation of the nuclear envelope to be distinguished from failure of the NPC permeability barrier (Figure 7A).

We first semi-permeabilized MEFs with digitonin, which is a weak nonionic detergent that selectively perforates the plasma membrane at low concentrations yet leaves the nuclear envelope intact (Colbeau et al., 1971; Adam et al., 1990). Incubation of these permeabilized MEFs with 70 kDa RITC-labeled and 500 kDa FITC-labeled dextran resulted in essentially no nuclear uptake of 500 kDa dextran, confirming digitonin permeabilization left the nuclear envelope intact. Over the timeframe of the assay, however, 70 kDa dextran leaked into a significantly higher percentage of nuclei from MEFs with OGT knockout (~30%) or inhibition (~40%), compared with control cells (~10%) (Figure 7B). Thus, decreased *O*-GlcNAc levels lead to a time-dependent loss of a number of natively *O*-GlcNAcylated Nups from the nuclear pore, which is reflected in a time-dependent breakdown of the selectivity barrier.

We next determined whether loss of *O*-GlcNAc also affected active transport through the NPC. To this end, we evaluated the effects of altered O-GlcNAc levels on the localization of transcription factor specificity protein 1 (Sp1), which is known to be highly *O*-GlcNAcylated with the glycosylation status regulating its stability (Jackson and Tjian, 1989; Han and Kudlow, 1997). Though levels of Sp1 were reduced in cells with OGT knockout or inhibition, the localization of Sp1 within the nucleus was similar to that in control cells. Proteasome inhibition restored Sp1 levels in cells having reduced *O*-GlcNAc, and the localization of Sp1 was still similar to that observed in control cells (Supplementary Figure S5). We also used a chimeric Rev-GFP-glucocorticoid receptor protein (RGG) (Love et al., 1998) to monitor the kinetics of import and export through the NPC. In the absence of dexamethasone, RGG is sequestered in cytoplasm, whereas in the presence of dexamethasone, RGG levels increase in the nucleus to reach a new dynamic equilibrium. Removing dexamethasone from the media leads to Rev-directed export of RGG to the cytoplasm and its cytoplasmic accumulation. In this study, RGG nuclear accumulation at initial stages of import was slower in cells with OGT inhibition than control cells (Supplementary Figure S6A). However, total levels of RGG in nuclei at equilibrium were equivalent in OGT inhibitor-treated cells and control cells. Interestingly, no difference was

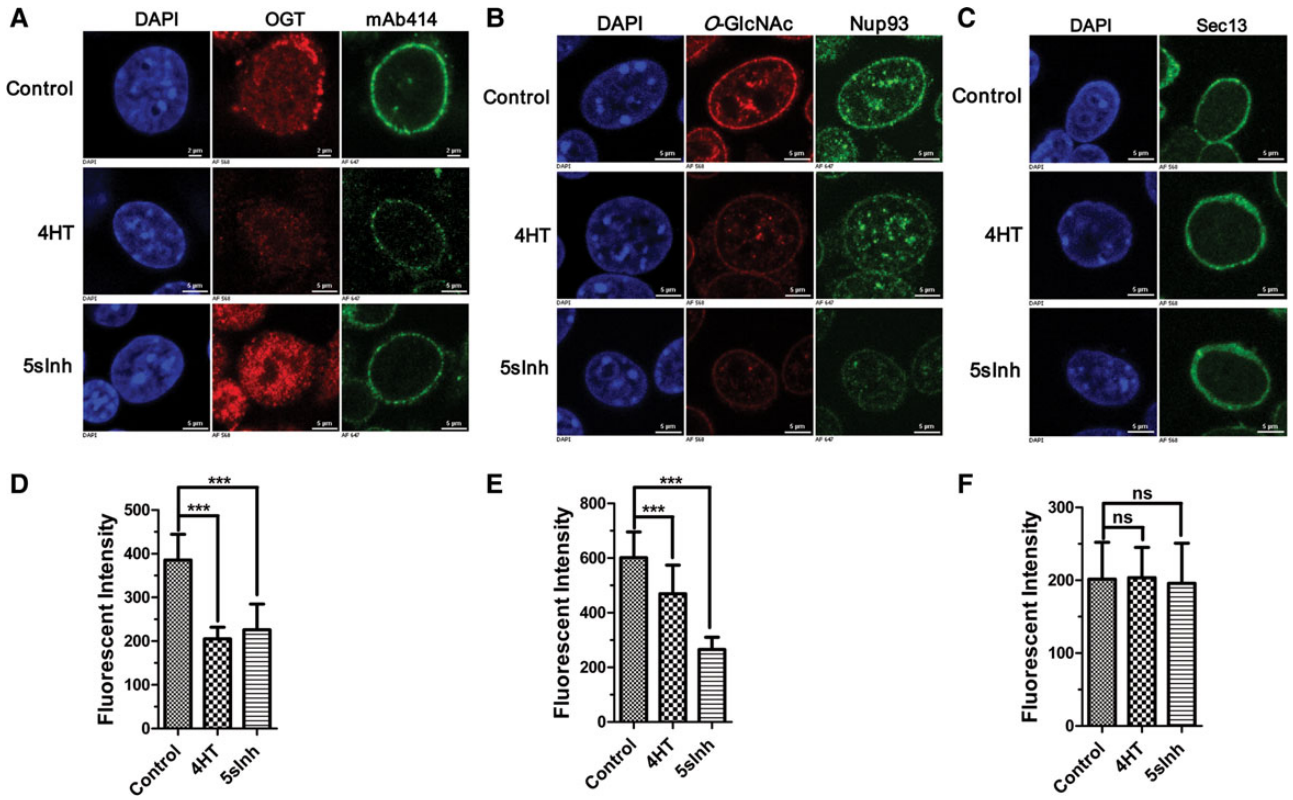

Figure 6 Loss of *O*-GlcNAc decreases the levels of Nups within the NPC. (**A**) Immunofluorescent microscopy of FG-rich Nups and OGT. Nuclei were isolated from cells with OGT knockout or inhibition for 3 days, and then fixed and stained with mAb414 and anti-OGT antibody. (**B**) Immunofluorescent microscopy of Nup93 and *O*-GlcNAc. Nuclei were isolated from cells with OGT knockout or inhibition for 5 days, and then fixed and stained with CTD110.6 and anti-Nup93 antibody. (**C**) Immunofluorescent microscopy of Sec13. Nuclei were isolated from cells with OGT knockout or inhibition for 5 days, and then fixed and stained with anti-Sec13 antibody. (**D**–**F**) The fluorescent intensity of FG-rich Nups (recognized by mAb414), Nup93, and Sec13 in **A**–**C** was quantified individually using image processing software NIS-Elements AR 3.1 (Nikon). Experiments were repeated for three times.

observed in export behavior of RGG between inhibitor-treated cells and control cells (Supplementary Figure S6B). These data suggest that active transport functions of the NPC are only slightly influenced by decreased *O*-GlcNAcylation and that defects in the selectivity filter do not manifest in the mislocalization of actively transported proteins.

Loss of O-GlcNAc causes defects in the selective permeability barrier of nuclear pores in post-mitotic cells

NPC deterioration has been proposed to be an important aging-related event in post-mitotic cells (D'Angelo et al., 2009; Hetzer, 2010). Scaffolding Nups of the NPC such as Nup93 have extremely long lifespans and neither exchange nor turn over in post-mitotic cells (D'Angelo et al., 2009). The expression of such scaffolding Nups and many others including Sec13, Nup62, Nup93, and Nup153 decreases once cells terminally divide (D'Angelo et al., 2009; Asally et al., 2011). We therefore speculated that loss of *O*-GlcNAc might increase the degradation of natively *O*-GlcNAcylated Nups and thereby lead to a loss of these Nups from the NPC, with the net consequence being compromise of the permeability barrier of the NPC in post-mitotic cells. Unlike in mammals, deletion of OGT is not lethal in *C. elegans*, and OGT knockout worms are viable and fertile (Hanover et al., 2005). We therefore used *C. elegans* to test this hypothesis. Because wild-type adult worms have dividing cells in their gonads, we used the temperature-sensitive sterile mutant strain SS104 *glp-4* (*bn2*) *I*, which at 15°C has normal morphology and is fertile but at 25°C loses its gonads and is sterile. The cells within adult *glp-4* mutant worms are therefore entirely post-mitotic at 25°C. We crossed OGT knockout mutant *ogt-1* (*ok430* or *ok1474*) with *glp-4* to make double mutants (*glp-4*; *ogt-1*), which lack *O*-GlcNAc (Supplementary Figure S7). We found that young (Day 1) adult worms in the process of losing *O*-GlcNAc displayed a trend toward a slight reduction of FG-Nups within NPCs and a similarly minor increase in the number of leaky nuclei. However, in older (Day 6) adult worms (*glp-4*; *ogt-1*), there was a significant loss of FG-Nups from the NPC and a striking increase in the percent of leaky nuclei compared with age-matched control worms (*glp-4*) (Figure 8). These data strongly suggest that loss of *O*-GlcNAc accelerates the deterioration of the NPC selectivity barrier in post-mitotic cells, which is proposed as a key event leading to accelerated aging (D'Angelo et al., 2009).

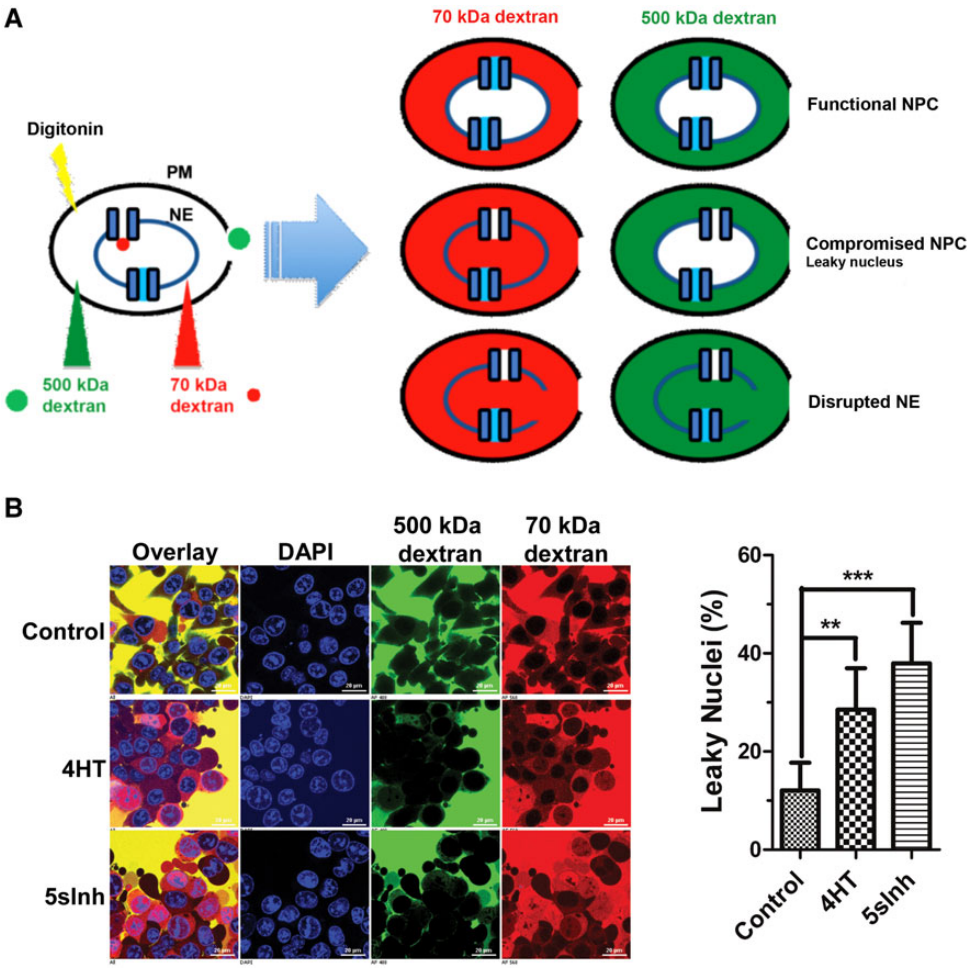

Figure 7 Loss of *O*-GlcNAc compromises NPC function. (**A**) Schematic of the experimental design of inert dextran exclusion assays. (**B**) Fluorescent dextran exclusion assays for inspecting NPC function in control cells, cells with OGT knockout for 2 days, and cells with OGT inhibition for 1 day. MEF cells were plated at ~15% confluency on cover slips. On the next day, one portion of the cells was incubated with 0.7 μM 4HT, and 4HT was removed after overnight incubation. The day after, culture media were replaced with fresh media for all the cells, and another portion of cells was incubated with 50 μM of 5sInh. After one more day, all the cells were semi-permeabilized using digitonin and incubated with red RITC 70 kDa and green FITC 500 kDa fluorescent dextrans. Then nuclear influx was analyzed by confocal microscopy. Images show each dextran in its original color. The percentage of leaky nuclei, which shows nuclear influx of 70 kDa but not 500 kDa dextran, was determined using image processing software NIS-Elements AR 3.1 (Nikon). Experiments were repeated for three times.

Discussion

Previous studies have shown that *N*-glycosylation of transmembrane Nup Pom152p influences nuclear protein import in yeast (Belanger et al., 2005). Little, however, has been uncovered about the role of glycosylation with *O*-GlcNAc, despite Nups having long been known to be among the most heavily *O*-GlcNAcylated proteins within mammalians cells (Holt and Hart, 1986; Davis and Blobel, 1987; Hanover et al., 1987; Holt et al., 1987). While this extensive *O*-glycosylation suggests that *O*-GlcNAc plays specific roles in the NPC, these putative roles have remained enigmatic. Previous reports have led to different proposals. Two lines of research have suggested that *O*-GlcNAc modification of Nups does not have obvious functional importance. Reconstitution of nuclear pores with components having galactosyl sugar residues added to *O*-GlcNAc did not alter NPC assembly or nuclear transport, suggesting that terminal *O*-GlcNAc structures were not essential (Miller and Hanover, 1994). Another report found that loss of OGT in *C. elegans* embryos and larvae had no effect on the levels of several natively glycosylated Nups, and several transcription factors were also observed to have normal localization (Hanover et al., 2005). Those data together suggest that *O*-GlcNAc does not play a role in the assembly of the NPC or active nuclear transport. However, given that cumulative loss of these glycosylated Nups from the NPC takes several days when OGT activity is blocked, perhaps the insensitivity of *C. elegans* embryos and larvae to the loss of *O*-GlcNAc stems from the rapid developmental program of *C. elegans* (Deppe et al., 1978). During this speedy period of swift cell division, high level production of Nups may ensure the fidelity of the expanding NPC population. In contrast to papers suggesting no functional role for glycosylation, others have suggested that *O*-GlcNAc plays an important role in the NPC, since binding of *O*-GlcNAc-targeted lectins hinders nuclear

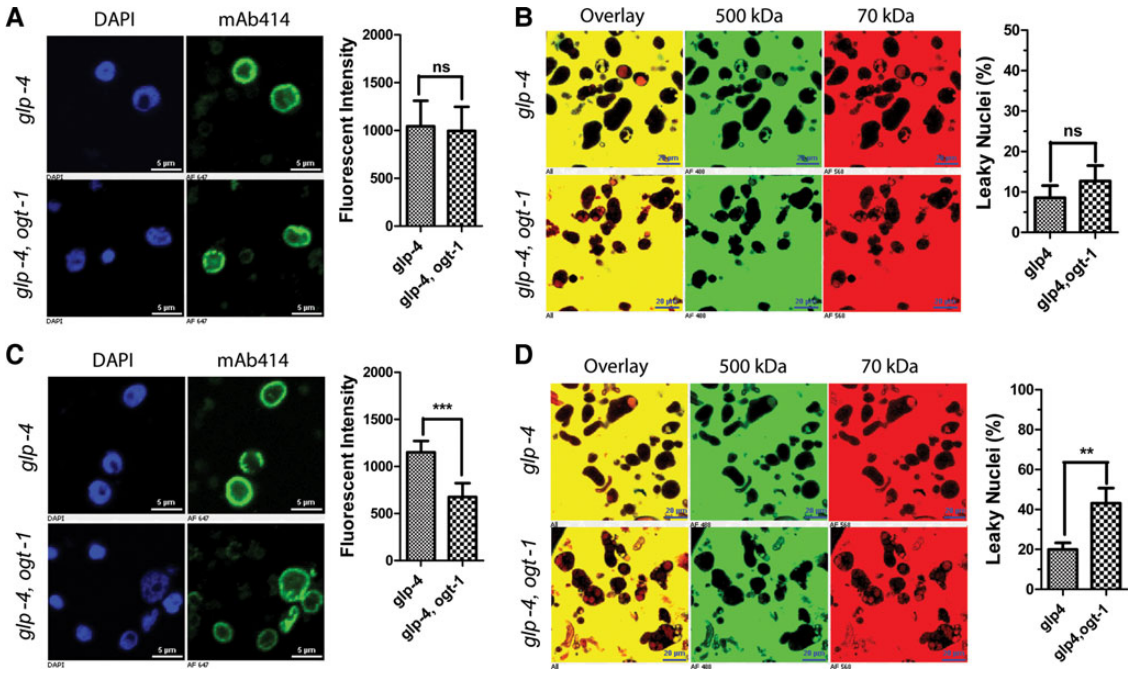

Figure 8 Loss of *O*-GlcNAc facilitates degradation of Nups and accelerates NPC deterioration in post-mitotic cells from *C. elegans*. (**A**) FG-Nups recognized by mAb414 antibody slightly reduced in nuclei from young (Day 1) adult worms with OGT knockout compared with control worms. (**B**) There was no significant difference in leaky nuclei percentage between young adult OGT mutant and control worms. (**C**) Levels of FG-Nups dropped remarkably in nuclei from old (Day 6) adult worms with OGT deletion compared with control worms. (**D**) Old adult worms losing *O*-GlcNAc had significantly more leaky nuclei than control worms.

transport (Finlay et al., 1987). This effect, however, is likely mediated by steric blockade of the channel by the *O*-GlcNAc-binding lectins (D'Angelo et al., 2006), rather than through specific roles played by *O*-GlcNAc. More recently, it has been found that the absence of *O*-GlcNAc on FG-Nups decreases the permeability of synthetic gels composed of FG-Nups (Labokha et al., 2013).

Here we find that decreases in *O*-GlcNAc levels, induced by either excision of *ogt* or inhibition of OGT, lead to a gradual time-dependent reduction of several Nups within the NPC, which under normal conditions are heavily *O*-GlcNAcylated. OGT knock-out and inhibition result in nearly identical effects on the stability of Nups and NPC function, revealing *O*-GlcNAc as a determinant of the stability of glycosylated Nups within the NPC. We further observe that the loss of these Nups leads to failure of the selectivity barrier in both mitotic and post-mitotic cells, in cell culture and in *C. elegans*, but only slightly affects active transport through the NPC. We therefore propose that a major functional role for *O*-GlcNAc on the NPC is to preserve NPC integrity and function, which is consistent with reports showing that depletion of various glycosylated Nups from isolated nuclei by using wheat germ agglutinin compromises the integrity of the NPC (Finlay and Forbes, 1990; Hulsmann et al., 2012).

We also find that *O*-GlcNAc acts to maintain the integrity of the NPC by hindering ubiquitylation of several Nups that are normally glycosylated. Inhibition or deletion of OGT led to the loss of *O*-GlcNAc from these Nups, increased downstream ubiquitylation, and consequent acceleration in their proteasomal degradation. Mutational deletion of known *O*-GlcNAc sites on Nup62 supports a direct role for *O*-GlcNAc in these processes and is consistent with a reduction of global *O*-GlcNAcylation not influencing the levels of non-*O*-GlcNAcylated scaffolding nucleoporins, Nup107 and Nup133 (Supplementary Figure S2A). Nevertheless, indirect mechanisms by which *O*-GlcNAc protects Nups beyond antagonism of ubiquitination may also be operative and are not excluded by these studies. For example, *O*-GlcNAc could stabilize Nups by increasing their biophysical stability or preventing their inappropriate aggregation. Further, these studies do not rule out indirect mechanisms caused by global reductions in *O*-GlcNAc levels, which may also contribute to destabilizing Nups and the permeability barrier of the NPC.

Over the 5-day timeframe of our studies, the core NPC assembly was unaffected by loss of *O*-GlcNAc, indicated by unchanged density of the NPC on the nuclear membrane and levels of scaffolding Nups Sec13, Nup107 and Nup133 within the NPC (Figure 6C and F, Supplementary Figures S2B and C, S4C and D). This variability in the rates at which different glycosylated Nups are lost may be attributable to the relatively sheltered location of the Nup107/160 complex that contains Sec13 within the NPC; in this position, it nestles against the nuclear membrane and is shielded by other Nups (Alber et al., 2007). Indeed, we note that *O*-GlcNAc is found on over 18 Nups but is most abundant on peripheral Nups (Supplementary Figure S8 and Table S1). *O*-GlcNAc on Nups is predominantly observed in regions that are not structurally defined except for Nup62, where residue T376 is in an α-helical domain (Solmaz et al., 2011), and Nup98, where residue T184 has been noted in a β-sheet structure (Ren et al., 2010). Accordingly, lower

O-GlcNAc levels most pronouncedly affect peripheral Nups that are in an exposed position and likely free to dissociate. It is possible, however, that more centrally positioned Nups, either glycosylated or not, could be lost from the NPC over longer periods of time within cells having decreased *O*-GlcNAc levels, as we see for the scaffolding Nup93 (Figure 6B and E). Such a loss might be precipitated by the steady loss of natively *O*-GlcNAcylated Nups in more exposed positions, which ultimately leads to the NPC being recognized as dysfunctional and being targeted for disassembly. This question remains an interesting problem to address, which requires a more detailed analysis of the effects of site-directed deletion of *O*-GlcNAcylation sites on a number of different Nups, coupled with the use of model systems enabling maintenance of cells lacking *O*-GlcNAc over periods longer than 5 days.

Our results provide a rationale for *O*-GlcNAc being conserved on the NPC of all multicellular eukaryotes studied to date. They also explain why these glycosylated Nups are such exceptional substrates for OGT and are constitutively modified. Our observations, in conjunction with the metabolic responsiveness of *O*-GlcNAc and recent recognition that the NPC composition varies from tissue to tissue (Ori et al., 2013), raise the intriguing question whether nutrient availability contributes to the regulation of nuclear pore composition through *O*-GlcNAc. The biological importance of the nuclear pore in aging has gained much attention, and it is interesting to speculate that *O*-GlcNAc may also influence NPC stability during aging. Recent studies have shown that within post-mitotic cells, most scaffold Nups are extremely long-lived, and these Nups are not exchanged nor turned over (D'Angelo et al., 2009). As cells age, some scaffold Nups that function as adaptors to anchor peripheral Nups containing FG repeats in the central channel, such as Nup93, accumulate damage to an extent where they no longer bind to NPC. Loss of these scaffold Nups from the NPC would lead to diminished levels of peripheral FG-Nups, which results in deterioration of the NPC selectivity barrier and subsequent age-related nuclear leakiness (D'Angelo et al., 2009). The situation in dividing cells is different; all NPC components are regularly replaced with newly synthesized proteins, ensuring NPC integrity (D'Angelo et al., 2009). Decreased cellular levels of *O*-GlcNAc may accelerate the aging process in post-mitotic cells by enabling more rapid degradation of Nups. Indeed, because most scaffold Nups within the NPC are not renewable after cell-cycle exit, loss of *O*-GlcNAc may be more profound in post-mitotic cells than in mitotic cells. Notably in this regard, *C. elegans* worms lacking *O*-GlcNAcylation have a shorter life span than wild-type ones, while worms lacking OGA and having elevated *O*-GlcNAc have a moderately extended lifespan (Love et al., 2010; Rahman et al., 2010). Though *O*-GlcNAc cycling impacts *C. elegans* lifespan by influencing signaling pathways as proposed (Love et al., 2010; Rahman et al., 2010), it seems possible that the protective role of *O*-GlcNAc may also be mediated by *O*-GlcNAc protecting the NPC. This view is consistent with our observations showing that NPC glycosylation is important for proper functionality of the NPC selectivity filter in mature *C. elegans*. Given the increasing importance of the nuclear pore in many aspects of cellular function and the pleiotropic effects of decreased *O*-GlcNAc levels, it is interesting to speculate that some effects arising from loss of *O*-GlcNAc might stem from impaired nuclear pore function. Here we provide a mechanistic explanation for the conserved glycosylation of the NPC and offer a clear rationale to drive future study into the pathophysiological roles of NPC glycosylation *in vivo*.

Materials and methods

Cell culture

Mouse embryonic fibroblast (MEF) cell line containing lentivirus encoding mutated estrogen receptor (mER)-Cre-2A-GFP construct was described previously (Kazemi et al., 2010). Cells were cultured in Dulbecco's modified Eagle's medium (DMEM; 1 g/L glucose) with 10% (*v*/*v*) fetal bovine serum (FBS) and 1% (*v*/*v*) penicillin/streptomycin at 37°C in a water-jacketed, humidified CO_2 (5%) incubator. Typically, cells were plated at 10%–25% confluency. Unless otherwise noted, Cre-recombinase was activated to knock out OGT through incubation with 0.7 μM 4-hydroxytamoxifen (4HT, Bioshop) 1 day after plating. To inhibit the OGT activity, Ac5SGlcNAc (5sInh) was added into cell culture to the final concentration at 50 μM. In the proteasome inhibitor tests, cells were incubated with 30 μM N-Acetyl-L-leucyl-L-leucyl-L-norleucinal (LLnL, Sigma) for 5 h before harvest. To inhibit deubiquitinases, cells were incubated with 5 μM deubiquitinase inhibitor PR619 (Sigma) for 5 h.

Worm strains

Strains N2 wild-type, the temperature-sensitive sterile mutant SS104 *glp-4 (bn2) I*, and OGT knockout mutants *ogt-1(ok430) III* and *ogt-1(ok1474) III* were purchased from the *Caenorhabditis* Genetics Center (CGC), Minneapolis, USA. Worms were grown at 15°C and maintained as described (Brenner, 1974). The mutant strains *ogt-1(ok430) III* and *ogt-1(ok1474) III* were backcrossed with N2 wild-type at least four times before crossing with SS104 *glp-4 (bn2) I* to produce double-mutant [*glp-4 (bn2); ogt-1(ok430)*] or [*glp-4 (bn2); ogt-1(ok1474)*].

Antibodies

CTD110.6 for detection of *O*-GlcNAc, and mAb414 detecting Nup62, Nup153, Nup214, and Nup358, were purchased from Covance. Other primary antibodies, including anti-OGT (H-300), anti-Nup93 (H-300), anti-Sec13 (N-16), anti-lamin A/C (H-110), anti-β-actin (C4), and anti-ubiquitin (P4D1), were all from Santa Cruz Biotechnology. All the secondary antibodies for western blot were from Li-Cor. All the secondary antibodies for immunofluorescent microscopy were purchased from Invitrogen. All antibodies were used as recommended by the suppliers.

Synthesis of OGT inhibitor Ac5SGlcNAc and cleavable triarylphosphine-biotin probe

Ac5SGlcNAc was synthesized as described previously (Gloster et al., 2011). Cleavable triarylphosphine-biotin probe was synthesized as described in Zhu et al. (2015).

Isolation of nuclei

MEFs were harvested and washed twice with PBS, and then incubated in hypotonic buffer (10 mM HEPES–KOH pH 7.5, 2 mM KCl,

1 mM DTT, 2 mM $MgCl_2$, 1 mM PMSF, 250 mM sucrose, and protease inhibitor cocktail mix) for 1 h. Swollen cells were homogenized with 20–30 strokes of a Dounce homogenizer (B-type pestle). Released nuclei were layered on top of hypotonic buffer and enriched by centrifugation at 500 *g* for 10 min and washed twice in hypotonic buffer. Finally, nuclei were resuspended in storage buffer (10 mM HEPES–KOH pH 7.5, 25 mM KCl, 2 mM $MgCl_2$, 250 mM sucrose, and protease inhibitors). Nuclei from worms on different days of adulthood were isolated as described (D'Angelo et al., 2009).

Nuclear dextran exclusion assays in semi-permeabilized cells

The method was adapted from Grote and Ferrando-May (2006). Briefly, after washing with cold PBS (4°C) for 1 min, MEFs grown on glass cover slips were semi-permeabilized with 20 μg/ml digitonin in permeabilization buffer (PB) (20 mM HEPES–KOH pH 7.5, 110 mM KOAc, 5 mM $Mg(OAc)_2$, 0.5 mM EGTA, protease inhibitor cocktail mix, and 250 mM sucrose) on ice for 3 min. Then semi-permeabilized cells were incubated twice with cold PB for 5 and 10 min, respectively. After incubation with transport buffer (TRB) (20 mM HEPES, 110 mM KOAc, 2 mM $Mg(OAc)_2$, 5 mM NaOAc, 0.5 mM EGTA, protease inhibitor cocktail mix, and 250 mM sucrose) for 5 min, semi-permeabilized cells were incubated with 0.6 mg/ml red RITC 70 kDa and green FITC 500 kDa fluorescent dextrans (Sigma-Aldrich) in TRB for 20–30 min in dark. Finally, nuclear influx of dextran was analyzed by confocal microscopy. Images show each dextran in its original color. The percentage of nuclei that showed nuclear uptake of the 70 kDa dextran but not the 500 kDa dextran was determined using image processing software NIS-Elements AR 3.1 (Nikon). Nuclei with a nuclear red fluorescent signal >20% and a nuclear green fluorescent signal <20% of the extracellular signal were considered leaky. Nuclei with a nuclear green fluorescent signal >20% of the extracellular signal were considered broken. Nuclei with a nuclear red fluorescent signal <20% and a nuclear green fluorescent signal <20% of the extracellular signal were considered intact (D'Angelo et al., 2009). Experiments were repeated three times. A minimum of 15 separate fields of vision covering ~600 nuclei were analyzed each time.

Other methods

Details for immunoblotting, pulse-chase experiments, cycloheximide-chase experiments, *in vitro* ubiquitination assays, preparation of the nuclear envelope fraction, immunofluorescence microscopy, overexpression of Nup62 in cells, immunoprecipitation of proteins, *in vitro* enzymatic de-*O*-GlcNAcylation, and import and export assays are described in the Supplementary Methods.

Supplementary material

Supplementary Material is available at *Journal of Molecular Cell Biology* online.

Acknowledgements

We thank Drs Jinkyo Suh and Harald Hutter (Simon Fraser University, Canada) for assistance with *C. elegans*, Dr Katharine Ullman (University of Utah, USA) for providing plasmid encoding the chimeric Rev-GFP-glucocorticoid receptor protein and Dr Valérie Doye (Institut Jacques Monod, France) for providing anti-Nup107 and Nup133 antibodies.

Funding

This work was supported by a Discovery Grant (grant no. RGPIN/298406-2010) from the Natural Sciences and Engineering Research (NSERC), and the Canadian Institutes of Health Research (CIHR) (grant no. MOP-123341). Y.Z. thanks the CIHR for support through a postdoctoral fellowship. D.J.V. acknowledges the kind support of the Canada Research Chairs Program for a Tier I Canada Research Chair in Chemical Glycobiology and NSERC for support as an E.W.R. Steacie Memorial Fellow. N.Z. acknowledges the support from the National Heart Lung and Blood Institute (P01HL107153).

Conflict of interest: D.J.V. is a cofounder of Alectos Therapeutics, a company involved in the development of OGA modulators for the treatment of Alzheimer's disease. D.J.V. serves as CSO and chair of the Scientific Advisory Board of Alectos Therapeutics.

References

Adam, S.A., Marr, R.S., and Gerace, L. (1990). Nuclear protein import in permeabilized mammalian cells requires soluble cytoplasmic factors. J. Cell Biol. *111*, 807–816.

Alber, F., Dokudovskaya, S., Veenhoff, L.M., et al. (2007). The molecular architecture of the nuclear pore complex. Nature *450*, 695–701.

Altun, M., Kramer, H.B., Willems, L.I., et al. (2011). Activity-based chemical proteomics accelerates inhibitor development for deubiquitylating enzymes. Chem. Biol. *18*, 1401–1412.

Asally, M., Yasuda, Y., Oka, M., et al. (2011). Nup358, a nucleoporin, functions as a key determinant of the nuclear pore complex structure remodeling during skeletal myogenesis. FEBS J. *278*, 610–621.

Belanger, K.D., Gupta, A., MacDonald, K.M., et al. (2005). Nuclear pore complex function in Saccharomyces cerevisiae is influenced by glycosylation of the transmembrane nucleoporin Pom152p. Genetics *171*, 935–947.

Boyce, M., Carrico, I.S., Ganguli, A.S., et al. (2011). Metabolic cross-talk allows labeling of O-linked beta-N-acetylglucosamine-modified proteins via the N-acetylgalactosamine salvage pathway. Proc. Natl Acad. Sci. USA *108*, 3141–3146.

Brenner, S. (1974). The genetics of Caenorhabditis elegans. Genetics *77*, 71–94.

Brohawn, S.G., Partridge, J.R., Whittle, J.R., et al. (2009). The nuclear pore complex has entered the atomic age. Structure *17*, 1156–1168.

Capelson, M., Liang, Y., Schulte, R., et al. (2010). Chromatin-bound nuclear pore components regulate gene expression in higher eukaryotes. Cell *140*, 372–383.

Colbeau, A., Nachbaur, J., and Vignais, P.M. (1971). Enzymic characterization and lipid composition of rat liver subcellular membranes. Biochim. Biophys. Acta *249*, 462–492.

Cronshaw, J.M., Krutchinsky, A.N., Zhang, W., et al. (2002). Proteomic analysis of the mammalian nuclear pore complex. J. Cell Biol. *158*, 915–927.

D'Angelo, M.A., and Hetzer, M.W. (2008). Structure, dynamics and function of nuclear pore complexes. Trends Cell Biol. *18*, 456–466.

D'Angelo, M.A., Anderson, D.J., Richard, E., et al. (2006). Nuclear pores form de novo from both sides of the nuclear envelope. Science *312*, 440–443.

D'Angelo, M.A., Raices, M., Panowski, S.H., et al. (2009). Age-dependent deterioration of nuclear pore complexes causes a loss of nuclear integrity in postmitotic cells. Cell *136*, 284–295.

Davis, L.I., and Blobel, G. (1987). Nuclear pore complex contains a family of glycoproteins that includes p62: glycosylation through a previously unidentified cellular pathway. Proc. Natl Acad. Sci. USA *84*, 7552–7556.

Debler, E.W., Ma, Y., Seo, H.S., et al. (2008). A fence-like coat for the nuclear pore membrane. Mol. Cell *32*, 815–826.

Deppe, U., Schierenberg, E., Cole, T., et al. (1978). Cell lineages of the embryo of the nematode Caenorhabditis elegans. Proc. Natl Acad. Sci. USA *75*, 376–380.

Dong, D.L., and Hart, G.W. (1994). Purification and characterization of an O-GlcNAc selective N-acetyl-beta-D-glucosaminidase from rat spleen cytosol. J. Biol. Chem. *269*, 19321–19330.

Elad, N., Maimon, T., Frenkiel-Krispin, D., et al. (2009). Structural analysis of the nuclear pore complex by integrated approaches. Curr. Opin. Struct. Biol. *19*, 226–232.

Finlay, D.R., and Forbes, D.J. (1990). Reconstitution of biochemically altered nuclear pores: transport can be eliminated and restored. Cell *60*, 17–29.

Finlay, D.R., Newmeyer, D.D., Price, T.M., et al. (1987). Inhibition of in vitro nuclear transport by a lectin that binds to nuclear pores. J. Cell Biol. *104*, 189–200.

Fujiki, R., Chikanishi, T., Hashiba, W., et al. (2009). GlcNAcylation of a histone methyltransferase in retinoic-acid-induced granulopoiesis. Nature *459*, 455–459.

Galy, V., Mattaj, I.W., and Askjaer, P. (2003). Caenorhabditis elegans nucleoporins Nup93 and Nup205 determine the limit of nuclear pore complex size exclusion in vivo. Mol. Biol. Cell *14*, 5104–5115.

Gambetta, M.C., Oktaba, K., and Muller, J. (2009). Essential role of the glycosyltransferase sxc/Ogt in polycomb repression. Science *325*, 93–96.

Gao, Y., Wells, L., Comer, F.I., et al. (2001). Dynamic O-glycosylation of nuclear and cytosolic proteins: cloning and characterization of a neutral, cytosolic beta-N-acetylglucosaminidase from human brain. J. Biol. Chem. *276*, 9838–9845.

Gloster, T.M., Zandberg, W.F., Heinonen, J.E., et al. (2011). Hijacking a biosynthetic pathway yields a glycosyltransferase inhibitor within cells. Nat. Chem. Biol. *7*, 174–181.

Grote, P., and Ferrando-May, E. (2006). In vitro assay for the quantitation of apoptosis-induced alterations of nuclear envelope permeability. Nat. Protoc. *1*, 3034–3040.

Han, I., and Kudlow, J.E. (1997). Reduced O glycosylation of Sp1 is associated with increased proteasome susceptibility. Mol. Cell. Biol. *17*, 2550–2558.

Hanover, J.A., Cohen, C.K., Willingham, M.C., et al. (1987). O-linked N-acetylglucosamine is attached to proteins of the nuclear pore. Evidence for cytoplasmic and nucleoplasmic glycoproteins. J. Biol. Chem. *262*, 9887–9894.

Hanover, J.A., Forsythe, M.E., Hennessey, P.T., et al. (2005). A Caenorhabditis elegans model of insulin resistance: altered macronutrient storage and dauer formation in an OGT-1 knockout. Proc. Natl Acad. Sci. USA *102*, 11266–11271.

Hanover, J.A., Krause, M.W., and Love, D.C. (2012). Bittersweet memories: linking metabolism to epigenetics through O-GlcNAcylation. Nat. Rev. Mol. Cell Biol. *13*, 312–321.

Hardiville, S., Hoedt, E., Mariller, C., et al. (2010). O-GlcNAcylation/phosphorylation cycling at Ser10 controls both transcriptional activity and stability of delta-lactoferrin. J. Biol. Chem. *285*, 19205–19218.

Hart, G.W., Slawson, C., Ramirez-Correa, G., et al. (2011). Cross talk between O-GlcNAcylation and phosphorylation: roles in signaling, transcription, and chronic disease. Annu. Rev. Biochem. *80*, 825–858.

Hetzer, M.W. (2010). The role of the nuclear pore complex in aging of post-mitotic cells. Aging (Albany NY) *2*, 74–75.

Hoelz, A., Debler, E.W., and Blobel, G. (2011). The structure of the nuclear pore complex. Annu. Rev. Biochem. *80*, 613–643.

Holt, G.D., and Hart, G.W. (1986). The subcellular distribution of terminal N-acetylglucosamine moieties. Localization of a novel protein-saccharide linkage, O-linked GlcNAc. J. Biol. Chem. *261*, 8049–8057.

Holt, G.D., Snow, C.M., Senior, A., et al. (1987). Nuclear pore complex glycoproteins contain cytoplasmically disposed O-linked N-acetylglucosamine. J. Cell Biol. *104*, 1157–1164.

Hulsmann, B.B., Labokha, A.A., and Gorlich, D. (2012). The permeability of reconstituted nuclear pores provides direct evidence for the selective phase model. Cell *150*, 738–751.

Iyer, S.P., Akimoto, Y., and Hart, G.W. (2003). Identification and cloning of a novel family of coiled-coil domain proteins that interact with O-GlcNAc transferase. J. Biol. Chem. *278*, 5399–5409.

Jackson, S.P., and Tjian, R. (1989). Purification and analysis of RNA polymerase II transcription factors by using wheat germ agglutinin affinity chromatography. Proc. Natl Acad. Sci. USA *86*, 1781–1785.

Jovanovic-Talisman, T., Tetenbaum-Novatt, J., McKenney, A.S., et al. (2009). Artificial nanopores that mimic the transport selectivity of the nuclear pore complex. Nature *457*, 1023–1027.

Kazemi, Z., Chang, H., Haserodt, S., et al. (2010). O-linked beta-N-acetylglucosamine (O-GlcNAc) regulates stress-induced heat shock protein expression in a GSK-3beta-dependent manner. J. Biol. Chem. *285*, 39096–39107.

Kreppel, L.K., Blomberg, M.A., and Hart, G.W. (1997). Dynamic glycosylation of nuclear and cytosolic proteins. Cloning and characterization of a unique O-GlcNAc transferase with multiple tetratricopeptide repeats. J. Biol. Chem. *272*, 9308–9315.

Labokha, A.A., Gradmann, S., Frey, S., et al. (2013). Systematic analysis of barrier-forming FG hydrogels from Xenopus nuclear pore complexes. EMBO J. *32*, 204–218.

Lenart, P., and Ellenberg, J. (2006). Monitoring the permeability of the nuclear envelope during the cell cycle. Methods *38*, 17–24.

Lenart, P., Rabut, G., Daigle, N., et al. (2003). Nuclear envelope breakdown in starfish oocytes proceeds by partial NPC disassembly followed by a rapidly spreading fenestration of nuclear membranes. J. Cell Biol. *160*, 1055–1068.

Li, B., and Kohler, J.J. (2014). Glycosylation of the nuclear pore. Traffic *15*, 347–361.

Love, D.C., Sweitzer, T.D., and Hanover, J.A. (1998). Reconstitution of HIV-1 rev nuclear export: independent requirements for nuclear import and export. Proc. Natl Acad. Sci. USA *95*, 10608–10613.

Love, D.C., Ghosh, S., Mondoux, M.A., et al. (2010). Dynamic O-GlcNAc cycling at promoters of Caenorhabditis elegans genes regulating longevity, stress, and immunity. Proc. Natl Acad. Sci. USA *107*, 7413–7418.

Lubas, W.A., Frank, D.W., Krause, M., et al. (1997). O-Linked GlcNAc transferase is a conserved nucleocytoplasmic protein containing tetratricopeptide repeats. J. Biol. Chem. *272*, 9316–9324.

Lupu, F., Alves, A., Anderson, K., et al. (2008). Nuclear pore composition regulates neural stem/progenitor cell differentiation in the mouse embryo. Dev. Cell *14*, 831–842.

Maimon, T., Elad, N., Dahan, I., et al. (2012). The human nuclear pore complex as revealed by cryo-electron tomography. Structure *20*, 998–1006.

Makhnevych, T., Lusk, C.P., Anderson, A.M., et al. (2003). Cell cycle regulated transport controlled by alterations in the nuclear pore complex. Cell *115*, 813–823.

Miller, M.W., and Hanover, J.A. (1994). Functional nuclear pores reconstituted with beta 1-4 galactose-modified O-linked N-acetylglucosamine glycoproteins. J. Biol. Chem. *269*, 9289–9297.

Mizuguchi-Hata, C., Ogawa, Y., Oka, M., et al. (2013). Quantitative regulation of nuclear pore complex proteins by O-GlcNAcylation. Biochim. Biophys. Acta *1833*, 2682–2689.

Natalizio, B.J., and Wente, S.R. (2013). Postage for the messenger: designating routes for nuclear mRNA export. Trends Cell Biol. *23*, 365–373.

Ori, A., Banterle, N., Iskar, M., et al. (2013). Cell type-specific nuclear pores: a case in point for context-dependent stoichiometry of molecular machines. Mol. Syst. Biol. *9*, 648.

Park, S.Y., Kim, H.S., Kim, N.H., et al. (2010). Snail1 is stabilized by O-GlcNAc modification in hyperglycaemic condition. EMBO J. *29*, 3787–3796.

Rahman, M.M., Stuchlick, O., El-Karim, E.G., et al. (2010). Intracellular protein glycosylation modulates insulin mediated lifespan in C. elegans. Aging (Albany NY) *2*, 678–690.

Raices, M., and D'Angelo, M.A. (2012). Nuclear pore complex composition: a new regulator of tissue-specific and developmental functions. Nat. Rev. Mol. Cell Biol. *13*, 687–699.

Ren, Y., Seo, H.S., Blobel, G., et al. (2010). Structural and functional analysis of the interaction between the nucleoporin Nup98 and the mRNA export factor Rae1. Proc. Natl Acad. Sci. USA *107*, 10406–10411.

Rodriguez-Bravo, V., Maciejowski, J., Corona, J., et al. (2014). Nuclear pores protect genome integrity by assembling a premitotic and Mad1-dependent anaphase inhibitor. Cell *156*, 1017–1031.

Ruan, H.B., Han, X., Li, M.D., et al. (2012). O-GlcNAc transferase/host cell factor C1 complex regulates gluconeogenesis by modulating PGC-1alpha stability. Cell Metab. *16*, 226–237.

Saxon, E., and Bertozzi, C.R. (2000). Cell surface engineering by a modified Staudinger reaction. Science *287*, 2007–2010.

Shen, D.L., Gloster, T.M., Yuzwa, S.A., et al. (2012). Insights into O-linked N-acetylglucosamine ([0–9]O-GlcNAc) processing and dynamics through kinetic analysis of O-GlcNAc transferase and O-GlcNAcase activity on protein substrates. J. Biol. Chem. *287*, 15395–15408.

Sinclair, D.A., Syrzycka, M., Macauley, M.S., et al. (2009). Drosophila O-GlcNAc transferase (OGT) is encoded by the Polycomb group (PcG) gene, super sex combs (sxc). Proc. Natl Acad. Sci. USA *106*, 13427–13432.

Solmaz, S.R., Chauhan, R., Blobel, G., et al. (2011). Molecular architecture of the transport channel of the nuclear pore complex. Cell *147*, 590–602.

Sood, V., and Brickner, J.H. (2014). Nuclear pore interactions with the genome. Curr. Opin. Genet. Dev. *25*, 43–49.

Starr, C.M., and Hanover, J.A. (1990). Glycosylation of nuclear pore protein p62. Reticulocyte lysate catalyzes O-linked N-acetylglucosamine addition in vitro. J. Biol. Chem. *265*, 6868–6873.

Stehno-Bittel, L., Perez-Terzic, C., and Clapham, D.E. (1995). Diffusion across the nuclear envelope inhibited by depletion of the nuclear Ca^{2+} store. Science *270*, 1835–1838.

Strambio-De-Castillia, C., Niepel, M., and Rout, M.P. (2010). The nuclear pore complex: bridging nuclear transport and gene regulation. Nat. Rev. Mol. Cell Biol. *11*, 490–501.

Tian, X., Isamiddinova, N.S., Peroutka, R.J., et al. (2011). Characterization of selective ubiquitin and ubiquitin-like protease inhibitors using a fluorescence-based multiplex assay format. Assay Drug Dev. Technol. *9*, 165–173.

Toyama, B.H., Savas, J.N., Park, S.K., et al. (2013). Identification of long-lived proteins reveals exceptional stability of essential cellular structures. Cell *154*, 971–982.

Van de Vosse, D.W., Wan, Y., Lapetina, D.L., et al. (2013). A role for the nucleoporin Nup170p in chromatin structure and gene silencing. Cell *152*, 969–983.

Vaquerizas, J.M., Suyama, R., Kind, J., et al. (2010). Nuclear pore proteins nup153 and megator define transcriptionally active regions in the Drosophila genome. PLoS Genet. *6*, e1000846.

Vinitsky, A., Michaud, C., Powers, J.C., et al. (1992). Inhibition of the chymotrypsin-like activity of the pituitary multicatalytic proteinase complex. Biochemistry *31*, 9421–9428.

Vocadlo, D.J. (2012). O-GlcNAc processing enzymes: catalytic mechanisms, substrate specificity, and enzyme regulation. Curr. Opin. Chem. Biol. *16*, 488–497.

Weis, K. (2002). Nucleocytoplasmic transport: cargo trafficking across the border. Curr. Opin. Cell Biol. *14*, 328–335.

Weis, K. (2003). Regulating access to the genome: nucleocytoplasmic transport throughout the cell cycle. Cell *112*, 441–451.

Wells, L., Slawson, C., and Hart, G.W. (2011). The E2F-1 associated retinoblastoma-susceptibility gene product is modified by O-GlcNAc. Amino Acids *40*, 877–883.

Wente, S.R., and Rout, M.P. (2010). The nuclear pore complex and nuclear transport. Cold Spring Harb. Perspect. Biol. *2*, a000562.

Yang, X., Su, K., Roos, M.D., et al. (2001). O-linkage of N-acetylglucosamine to Sp1 activation domain inhibits its transcriptional capability. Proc. Natl Acad. Sci. USA *98*, 6611–6616.

Yang, W.H., Kim, J.E., Nam, H.W., et al. (2006). Modification of p53 with O-linked N-acetylglucosamine regulates p53 activity and stability. Nat. Cell Biol. *8*, 1074–1083.

Zhu, Y., Liu, T.W., Cecioni, S., et al. (2015). O-GlcNAc occurs cotranslationally to stabilize nascent polypeptide chains. Nat. Chem. Biol. *11*, 319–325.